INTENSITY INCREASES OF ACTIN LAYER-LINES ON ACTIVATION OF THE *LIMULUS* MUSCLE

Y. MAÉDA,* C. BOULIN,‡ A. GABRIEL,§ I. SUMNER,‖ AND M. H. J. KOCH*

**EMBL, Hamburg Outstation, c/o DESY, D-2000 Hamburg 52, Federal Republic of Germany; ‡EMBL Heidelberg, D-6900 Heidelberg, Federal Republic of Germany; §EMBL Grenoble Outstation, c/o ILL, 156X, F-38042 Grenoble-Cedex, France; and* SERC *Daresbury Laboratory, Warrington, WA4 4AD, United Kingdom*

ABSTRACT Small angle x-ray diffraction patterns were recorded from isometrically contracting *Limulus* (horseshoe crab) telson levator muscle using a multiwire proportional-area detector on the storage ring DORIS. In the pattern a substantial increase in intensity is observed on the thin-filament-associated layer-line at 1/38 nm^{-1} (the first actin layer-line) with a maximum increase at a radial spacing of $R = 0.07$ nm^{-1} but there is a much smaller change in the intensity of the 5.9-nm layer-line, which also arises from the thin filament structure. The results suggest that during contraction the myosin heads, presumably being attached to the thin filaments, are arranged along the long-stranded helical tracks of the thin filaments but that the spatial relationship between the heads and the actin monomers varies. Intensity increases have also been observed (Maéda et al., manuscript in preparation) in the part of the patterns from frog muscle and barnacle muscle, which are attributable to the first actin layer-line. It is thus likely that the intensity increase of the first actin layer-line on the *Limulus* pattern is associated not with structural features which are special to *Limulus* muscle, but with the tension generating processes that are shared by muscles in general.

INTRODUCTION

It is widely believed that in activated muscle the contracting force is generated by repetitive interaction of the head portion of myosin molecules with actin molecules in the thin filament. In resting muscle, the mass distribution of the myosin heads is governed by the symmetry of the thick filament structure, whereas on activation, the repetitive interaction implies that the arrangement of the heads must also depend on that of the actin in the thin filaments. The thin-filament-associated reflexions from activated muscles thus, in principle, contain information about the arrangement, configuration, and number of heads attached to the thin filaments or at least sterically influenced by them.

It is thus surprising that in the pattern from contracting frog muscle, no intensity increase assignable to binding of the myosin heads to the thin filaments has been detected (Huxley et al., 1982; Huxley et al., 1985). For this reason, we examined the pattern from contracting *Limulus* telson levator muscle using an area detector. The pattern of *Limulus* muscle has fewer, less-extended and less-intense thick-filament-associated layer-lines than the frog pattern. This makes it much easier to isolate the intensities of the thin filament associated reflections from those of the thick filament structure.

Our experiments indicate that in the *Limulus* pattern there is indeed a substantial intensity increase on the first actin layer-line and a much smaller change on the layer-line at 1/5.9 nm^{-1}. This suggests that during contraction the myosin heads remain arranged along the long-stranded helical tracks of the thin filaments but that the spatial relationship between these heads and the actin monomers varies.

The present results also demonstrate the great advantage of area detectors over linear ones for the study of the weaker parts of the diffraction pattern of muscle. Except for some early experiments by Huxley et al. (1980) using a TV detector, all time-resolved diffraction data on contracting muscle had hitherto been recorded with linear detectors. In practice, this has meant that a very large number of experiments had to be performed to correlate the changes in various parts of the diffraction pattern. It is, however, almost impossible to obtain detailed information about the intensity distribution on the layer-lines. Although many of the experiments with a fine time resolution can still only be done with fast linear detectors, there is a definite advantage in using area detectors for measurements on the weaker parts of the pattern for which there are no count-rate limitations.

MATERIALS AND METHODS

Muscles

Telson levator muscles of the horseshoe crab (*Limulus polyphemus*) were used. The muscles were mounted in Perspex cells with Mylar windows in oxygenated Ringer's solution for seawater animals at 12–13°C. The muscles were stimulated by applying a bipolar sinusoidal electric field through platinum plates parallel to the muscle length. After each experiment, the cross-sectional area of the muscle was calculated from the

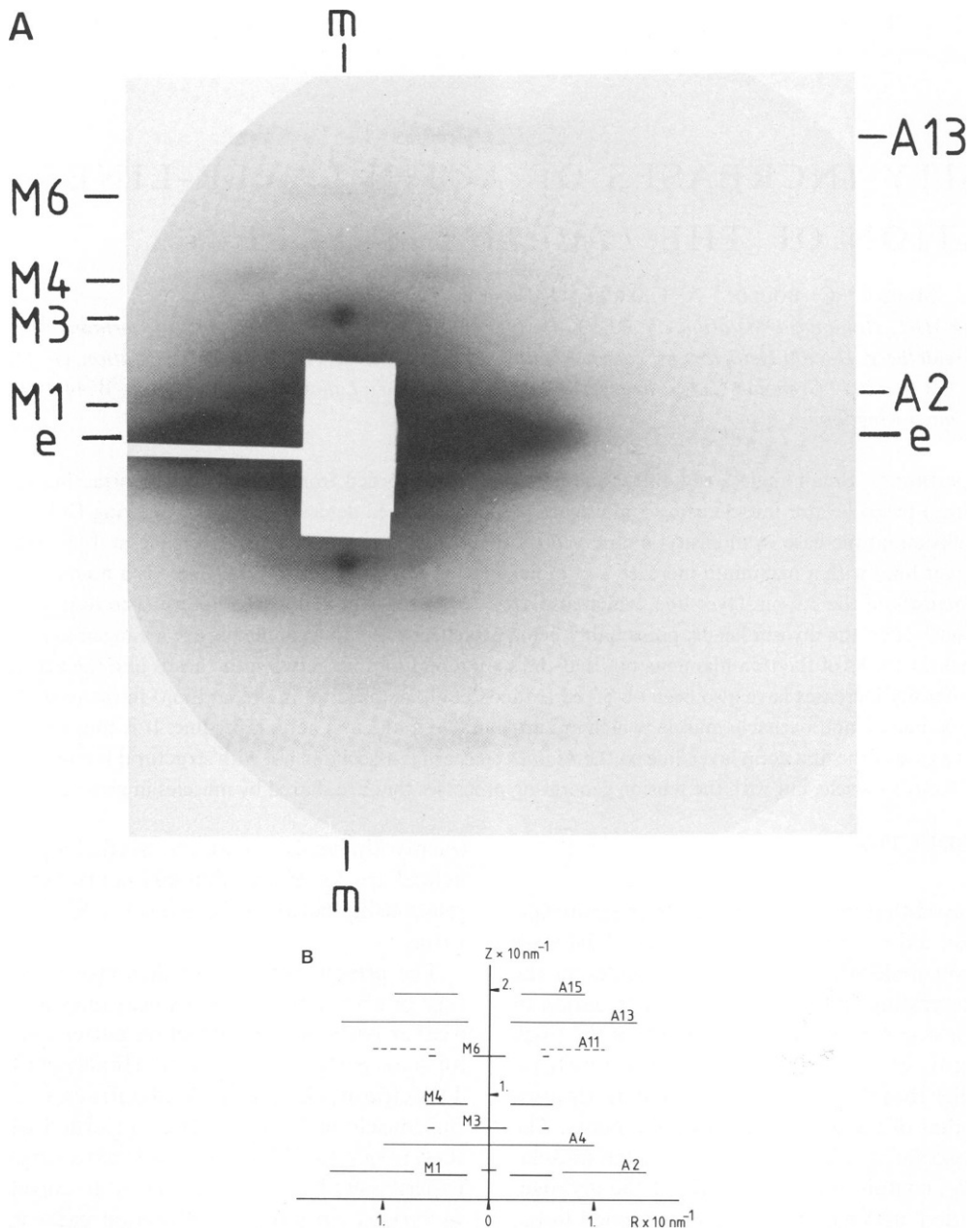

FIGURE 1 X-ray diffraction from *Limulus* telson levator muscle in the resting state. (*A*) The pattern recorded on x-ray film. (*m*: meridian; *e*: equator). (*B*) Schematic representation of the layer-line reflexions. The ordinate corresponds to the axial spacing and the abscissa to the radial spacing (in nm^{-1}). The thick filament associated reflexions are labeled with *M*, the thin filament associated reflexions with *A*. For nomenclature of the reflexions see the text.

weight and the length of the muscle, assuming a specific gravity of 1.05. The muscle length was adjusted to a sarcomere length of 8 μm to 9 μm to generate the maximum tension. Data from muscles that generated an initial maximum tension below 3.5 kg/cm^2 were rejected.

Experimental Protocol

Electric stimulations with a duration of 2.25 s were applied every 2 min, giving rise to isometric tetanic contractions. X-ray diffraction patterns were recorded in three successive time slots (I–III) synchronized with the onset of the stimulation ($t = 0$) as follows: I: (-2 s $< t <$ 0 s) to obtain a pattern of the relaxed muscle; II: (0 s $< t <$ 0.25 s) for a pattern during the tension rise; III: (0.25 s $< t <$ 2.25 s) for a pattern during activation. After each session of 25 contraction cycles, data collection was interrupted and the contents of the memory were dumped on disk. After analysis of the quality of the patterns and the extent of the changes, the data from the first two sessions were usually averaged. At the end of the second session, muscles generated a tension of 60–70% of the initial level under these conditions of exposure to the intense x-ray beam.

X-ray Optics

The data were recorded on the X33 camera of the EMBL in the HASYLAB on the storage ring DORIS of the Deutsches Elektronen Synchroton (DESY) in Hamburg. The camera has a triangular germanium monochromator focusing in the horizontal direction followed by a

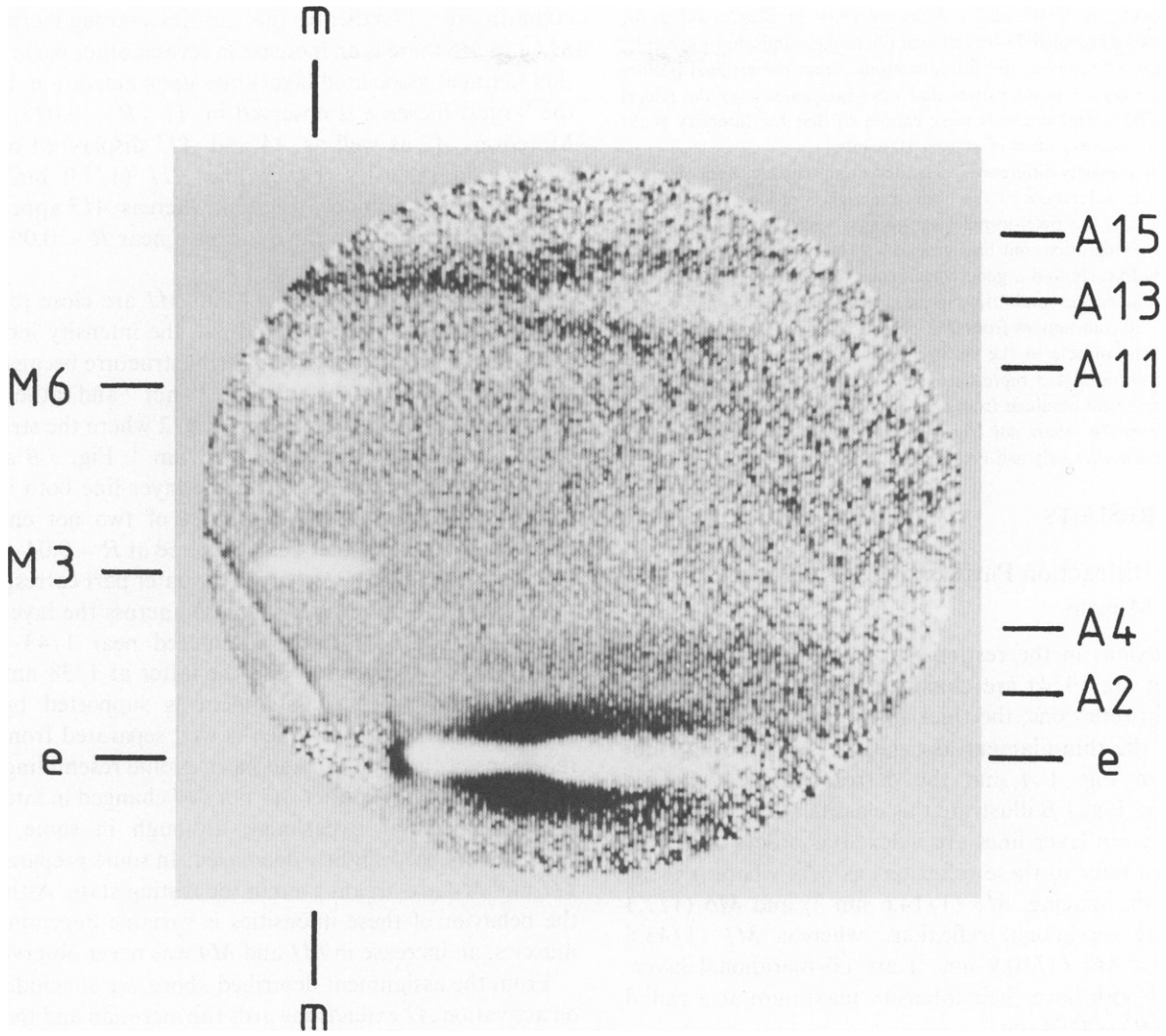

FIGURE 2 A difference pattern showing the distribution of intensity changes in the pattern of *Limulus* muscle upon activation. This pattern was obtained by subtracting the pattern from the resting muscle from that of the same muscle during isometric contraction. The bright contrast indicates the areas where the intensity increases more than in the surrounding parts upon activation, whereas the dark contrast corresponds to a decrease. (*m*: meridian; *e*: equator).

totally reflecting segmented quartz mirror that focuses in the vertical direction. Details of the design of this type of instrument have been described elsewhere (Hendrix et al., 1979; Bordas et al., 1980; Koch and Bordas, 1983). The x-ray wavelength used was 1.5 Å. During the experiments the storage ring was operated at 5 GeV with a maximum current of 40 mA.

Area Detector, Data Acquisition, and Evaluation System

The detector has an active area of 200 × 200 mm covered by a 1-mm thick beryllium window. The wire planes consist of stainless steel wires, 10 μm in diameter for the anode and 20 μm in diameter for the cathodes, with 1 mm spacing. The gap between the anode plane and each of the two cathodes is 5 mm. The detector was operated at 4.5 kV with a 70:30 argon/CO_2 mixture which is flowed at a pressure of one atmosphere. The overall efficiency of the system taking into account the losses in the Be-window is ~12%. During the experiments the total count rate over the whole detector area monitored on the anode did not exceed 2.0×10^5 counts/s.

The readout system was similar to the one described by Boulin et al. (Boulin et al., 1982) except that commercially available CAMAC time-to-digital convertors (#4210, LeCroy-Geneva) with 2-ns resolution were used. The digital X and Y addresses were combined in a purpose-built module and passed on to the controller of a CAMAC histogramming memory (see S.E.R.C. Daresbury Laboratory Technical Manual, EC601 Memory Controller, CSE:Instrumentation:M03) allowing up to eight frames of 256 × 256 pixels to be stored. The data collection sequence was controlled by a programmable time-frame generator. The muscle tension and intensity of the primary beam were recorded simultaneously with the x-ray data collection and stored in a calibration channel unit (Boulin, 1982). The data acquisition programs written in CATY (Golding, 1982) were run on an LSI 11/2 auxiliary crate controller linked to PDP 11/45 computer via a CAMAC serial highway (Clout et al., 1978). For display and analysis, a CAMAC video controller and frame buffer (Boulin et al., unpublished) driven by a FORTRAN interactive image processing program package (Koch, unpublished) was used on a VAX 11/750 computer.

Intensity profiles along the layer-lines were obtained as follows. A value for each pixel was summed up in the direction parallel to the equator over the lateral intervals of 3 to 5 pixels, which correspond to

lateral spacing of 0.007 nm^{-1}. Thus intensity profiles crossing the layer-lines were provided. Subtraction of the backgrounds, fit by eye or by the program with polynomial fitting routines, from the original profiles provided the layer-line intensities that were integrated over the lateral intervals. The lateral intervals were chosen so that the intensity peaks along the layer-lines consist of at least 10 points.

Profiles of intensity differences, activated minus resting, were obtained by taking the differences of the above-mentioned profiles. For the *A2* layer-lines only, the pixel-to-pixel subtraction was also made and was followed by integration and background subtraction. The two methods gave results that showed a good coincidence, suggesting that the errors involved in the background fitting in the steep region are not significant.

Data of 220 contractions from four preparations were added up. In the pattern of the muscle in the resting state, the peaks of the intensity profiles for *A2* and *A13* represent $\sim 5 \times 10^4$ counts for one-half of the pattern. The result obtained from each preparation was not significantly different from the others nor from the cumulative result, although the cumulative one obviously had better statistics.

RESULTS

Diffraction Pattern from the Resting Muscle

The reflexions in the resting pattern of *Limulus* muscle (Wray et al., 1974) are classified into three groups; the equatorial reflexions, the thick-filament associated reflexions and the thin-filament associated reflexions. The film pattern in Fig. 1 *A* and the corresponding schematic diagram in Fig. 1 *B* illustrate this classification.

The myosin layer-lines are indexed as orders of 1/43.8 nm^{-1}. We refer to these reflexions as *Mn*, where *n* is the order of the spacing. *M3* (1/14.6 nm^{-1}) and *M6* (1/7.3 nm^{-1}) are meridional reflexions, whereas *M1* (1/43.8 nm^{-1}) and *M4* (1/10.9 nm^{-1}) are off-meridional layer-lines that both have their intensity maximum at a radial spacing (*R*) of 0.04 nm^{-1}.

The thin filament associated layer-lines are indexed as orders of 1/77 nm^{-1} and are referred to as *An* following the same convention as above. In the resting state, the layer-lines *A2* (1/38 nm^{-1}), *A4* (1/19 nm^{-1}), *A13* (1/5.9 nm^{-1}), and *A15* (1/5.1 nm^{-1}) are observed in the small angle region.

Intensity Changes of Thin-Filament-Associated Layer-lines

Fig. 2 shows a difference pattern obtained by subtracting the pattern of the resting state from that of the same muscle during contraction. The pattern shows only one quadrant of the whole pattern. The bright (dark) contrast indicates areas where, upon activation, the intensity increases (decreases) more. Even small intensity changes in the layer-line are easily noticed in these difference patterns. The intensity changes are presented more quantitatively in Figs. 3 *A* and *B*, which have been obtained from the whole pattern, four quadrants being averaged. Fig. 3 *A* shows the intensity profiles of the thin filament associated layer-lines from the muscle in resting and isometrically contracting states. The difference in the profile of the two states in Fig. 3 *B* indicates that besides a strong increase in *M3* and *M6* there is an increase in several other parts of the thin filament associated layer-lines upon activation. By far the largest increase is observed in *A2* $\sim R = 0.075$ nm^{-1}. Moreover, *A2* as well as *A4* and *A15* display an overall increase in intensity. Layer line *A11* (1/7.0 nm^{-1}) is observed only during contraction, whereas *A13* appears to increase in intensity in the outer part near $R = 0.09$–0.15 nm^{-1} (but see below).

Although the layer-lines *A2* and *M1* are close to each other as shown in Fig. 1 *B* and 3*A*, the intensity increase can be attributed to the thin filament structure because it is centered on the axial spacing at 1/38 nm^{-1} and rather than 1/43.8 nm^{-1}. This is best seen in Fig. 2 where the stripe of white contrast is centered at 1/38 nm^{-1}. Fig. 3 *B* shows that the intensity profiles along the layer-line both in the resting and activated states consist of two not entirely resolved peaks. The inner peak centered at $R = 0.04$–0.045 nm^{-1} is assigned to *M1*, whereas the outer part corresponds to *A2* since the intensity distribution across the layer-line indicates that the former is centered near 1/43 nm^{-1} axially at $R = 0.04$ nm^{-1} and the latter at 1/38 nm^{-1} at $R = 0.1$ nm^{-1}. This assignment is supported by the intensity profile of *M4*, which is well separated from any reflexions of the *A* group and has a profile resembling that of the inner peak. Neither *M1* nor *M4* changed in intensity in this particular experiment although in some other experiments both slightly decreased. In some preparations *M1* and *M4* are absent even in the resting state. Although the behavior of these intensities is variable depending on muscles, an increase in *M1* and *M4* was never observed.

From the assignment described above, we conclude that on activation *A2* extends towards the meridian and that the intensity maximum shifts from $R = 0.1$ nm^{-1} in the resting state to $R = 0.08$–0.09 nm^{-1} on activation. This lateral shift of the *A2* peak was taken as significant for the following reasons. First, the intensity profiles (Fig. 3) were reproducible and not affected significantly by the background fitting (see Materials and Methods). Second, the intensity increased most at $R = 0.07$ nm^{-1} (Fig. 3 *B*), which is significantly different from $R = 0.1$ nm^{-1} where *A2* has its intensity maximum in the resting state. Third, the shift was easily recognized by visual inspection of the two dimensional patterns on a TV screen.

The outer part of *A13* appears to increase substantially but closer examination of the difference pattern in Fig. 2 indicates that the layer-line is narrower in the axial direction in the activated state than in the resting state. This is confirmed by inspecting the intensity profiles crossing the layer-lines. Therefore, the apparent intensity increase at this position may well be due to incorrect subtraction of the background, i.e., the layer-line in the resting pattern is so wide in the axial direction that the intensity associated with it may be underestimated. The change in width suggests that the filaments are better oriented in activated muscle and this could also explain the

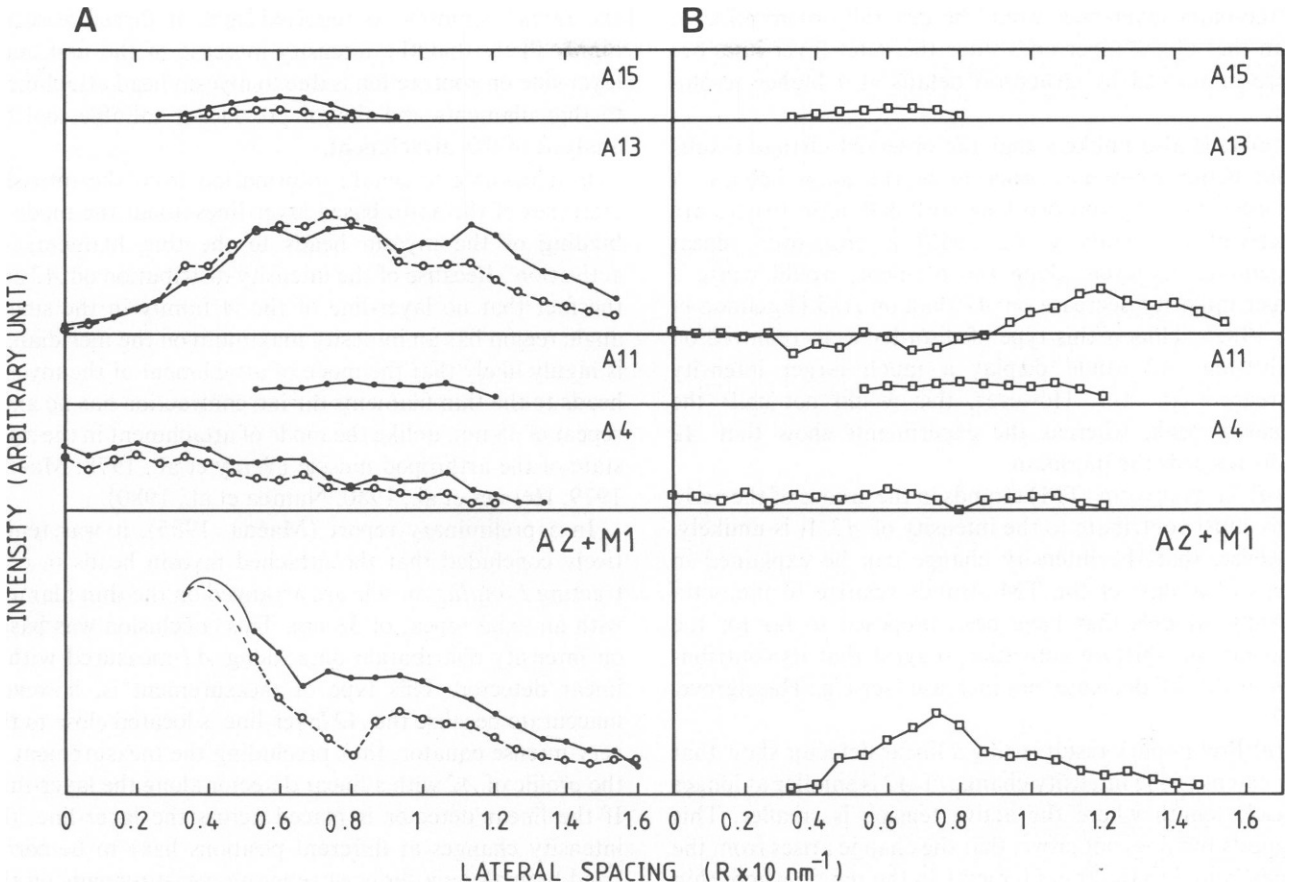

FIGURE 3 Intensity distributions along the thin filament associated layer-lines in the pattern of *Limulus* muscle shown in Fig. 2. (*A*) The intensity distributions of the muscle in the resting state (○) are compared with those of the same muscle in the activated state (●). (*B*) Difference between the distributions from the contracting muscle and the resting muscle obtained from spectra shown in (*A*). The abscissa is the radial spacing *R*. The origins ($R = 0$) are on the meridian.

apparent axial shift of the inner part of *A13* towards the origin, as indicated by the dark stripe on the far side of the layer-line in Fig. 2. It is not yet clear, however, whether the filaments themselves are better oriented or whether the orientation of the fibers is improved on activation.

In separate experiments using a fast linear detector (manuscript in preparation), *A*13 increases from 100 to 140% and *A*2 increases from 65 to 205% upon activation, where the peak height of *A*13 in the resting state is taken as 100%. In contrast, in the present experiments, *A*13 shows almost no increase and *A*2 from 65 to 140%. The smaller changes measured here are probably due to fatigue of the preparations as more frequent and more prolonged contractions were required for the measurements. Therefore, it may be concluded that, apart from the effect of improved orientation which has been described above, *A*13 does undergo an overall intensity increase, however, the extent of this change is much smaller than that of *A*2.

Although the intensity of *A4*, *A11*, and *A15* clearly increase relative to the resting levels, the absolute increases are much smaller than those of *A2*. Also, the intensity profiles of *A4* and *A15* do not significantly change on activation.

Changes in Myosin Reflexions

In the *Limulus* pattern, the meridional myosin reflexions *M3* and *M6* both increase in intensity and in width across the meridian, as in the frog pattern (Huxley et al., 1980; Yagi et al., 1981; Huxley et al., 1982) but no axial shift is observed. Details of the changes of the myosin reflexions will be described elsewhere.

DISCUSSION

Origin of the Intensity Change of *A2*

The intensity increase of the *A2* layer-line observed on activation in the pattern of *Limulus* muscle can be interpreted in terms of binding of the myosin heads to the thin filaments on the basis of the following arguments.

(*a*) Although the intensity increase could result from improved orientation of the thin filaments on activation this could not explain the changes in the intensity distribution of *A2*.

(*b*) It is unlikely that the observed change of *A2* arises from conformational changes of the actin monomers. If the overall shape of the actin monomers changed, the intensity

of the outer layer-lines would be generally more affected than that of the inner ones since the outer layer-lines are more influenced by structural details at a higher resolution.

(*c*) It is also unlikely that the observed change results from better rotational ordering of the actin helices. A disorder whereby the two long stranded actin helices are intertwined irregularly, i.e., with a cross-over repeat depending on levels along the filament, would cause a larger intensity decrease on *A2* than on *A13* (Egelman et al., 1982). Thus if this type of disorder were removed on activation, *A2* would display a much larger intensity increase than *A13*. However, this would not shift the intensity peak, whereas the experiments show that *A2* shifts towards the meridian.

(*d*) Tropomyosin (TM) strands in the groove of the actin helix must contribute to the intensity of *A2*. It is unlikely, however, that the intensity change can be explained in terms of a shift of the TM strands relative to the actin strands. Models that have been proposed so far for the tropomyosin shift on activation suggest that its contribution to *A2* will decrease, not increase (see e.g., Haselgrove, 1973).

(*e*) Preliminary results using a linear detector show that the extent of the intensity change of *A2* is smaller at longer muscle length where the active tension is smaller. This suggests but does not prove, that the change arises from the heads bound to the thin filaments in the region where thin and thick filaments overlap.

(*f*) The shift of the intensity maxima towards the meridian can be explained in terms of the extra mass from the myosin heads located on the outer part of the long-stranded actin helices shifting the center of mass of the strands outward.

At the present stage, it could be argued that at least a part of the intensity increase of the first layer-line is contributed by the myosin heads bound to the thin filaments. However, the possibility that some unattached heads that are under the influence of the bound heads also contribute to the intensity increase cannot be excluded.

In x-ray diffraction patterns, so far, none of the measured intensity changes of reflexions have been interpreted in terms of the binding of the myosin to the thin filaments during contraction. The change in the intensity distribution on the equator does not distinguish between the myosin heads actually binding to the thin filaments, or staying in their vicinity (Haselgrove and Huxley, 1973). Recently, Matsubara and his colleagues (Matsubara et al., 1984) interpreted the intensity increase of the 5.9-nm layer-line in the frog pattern as a strong evidence for the actomyosin attachment. However, there is evidence that not all the change of this layer-line can be interpreted in terms of the binding (Huxley et al., 1985). Moreover, it is likely that in general the intensity change of this layer-line is much smaller than that of the first layer-line. This is the case in the *Limulus* muscle as reported here. It therefore seems highly likely that the intensity increase of the first actin layer-line on contraction is due to myosin head attachment to thin filaments and that it provides a suitable tool for analysis of this attachment.

Is it possible to obtain information from the intensity increases of the actin based layer-lines about the mode of binding of the myosin heads to the thin filaments on activation? Because of the intensity distribution on *A2* and the fact that no layer-line of the *A* family in the small-angle region has an intensity maximum on the meridian, it is highly likely that the mode of attachment of the myosin heads to the thin filaments during contraction has no axial repeat of 38 nm, unlike the mode of attachment in the rigor state of the arthropod muscle (Wray et al., 1978; Maéda, 1979; Holmes et al., 1980; Namba et al., 1980).

In a preliminary report (Maéda, 1985), it was tentatively concluded that the attached myosin heads in contracting *Limulus* muscle are arranged on the thin filament with an axial repeat of 38 nm. This conclusion was based on intensity distribution data along *A2* measured with a linear detector. This type of measurement is, however, inaccurate because the *A2* layer-line is located close to the very intense equator, thus precluding the measurement of the profile of *A2* with a linear detector along the layer-line. If the linear detector is placed across the layer-line, the intensity changes at different positions have to be correlated by making a series of separate measurements on the same specimen or on different ones. This is very difficult since the extent of activation and hence also the intensity change is not reproducible as the specimen continuously degrades during a session and different preparations can be activated to different extents. The previous data are not consistent with the present ones, shown in Fig. 3, which are more reliable and reproducible.

Explanation of the Small Change of *A13*

At first sight, it might be puzzling that the substantial increase and the lateral shift of the *A2* layer-line is associated with a much smaller intensity increase of the *A13* layer-line. Binding the extra mass to each actin monomer can cause substantial intensity increase of the 5.9-nm (*A13*) layer-line and/or the 5.1-nm (*A15*) layer-line. However, noting that the spatial resolution associated with each layer-line are different from each other, the observation can be easily accounted for.

The layer-line *A2* is related to the mass distribution along the long-pitch (77 nm) two-stranded helices of the thin filament. The layer-line *A13* is related to that of the short-pitch (5.9-nm) one-start helix. A structure in which the 5.9-nm helical track is prominent would give rise to a strong 5.9-nm layer-line (*A13*). Therefore the large increase in intensity on *A2* and the much smaller change on *A13* can be explained by a regular arrangement of the

heads on the thin filament in a configuration that emphasizes the long-stranded helices, but not the 5.9-nm helix. In other words, the heads are relatively well aligned on the tracks of the long-stranded helices but randomly located relative to the track of the 5.9-nm pitch helix.

The results reported here place restrictions in modelling the configuration of the actomyosin complex in contracting muscle, although no particular model can be chosen at the present stage.

Significance of the Intensity Increase of *A2*

It is of great interest to determine if the intensity increase of the actin first layer-line (*A2*) on activation is associated with some specific structural features of the *Limulus* muscle, or if it is common to all muscle species. Recently, in the x-ray diffraction pattern from the frog muscle, an axial shift of the first layer-line has been observed on activation. Since the first actin layer-line is superimposed on the first myosin layer-line in the frog pattern, this strongly suggests that there is also an intensity increase of the first actin layer-line (Maéda, Y., and H. Huxley, unpublished observations). In the pattern from barnacle muscle, where no myosin-associated layer-lines are observed, there is a substantial intensity increase on the first actin layer-line upon activation (Maéda, Y., P. Griffiths, and C. Ashley, manuscript in preparation). Finally, by employing the rapid-freezing electron-microscope technique, Tsukita and Yano (1985) reported the intensification of the 37-nm layer-line in the optical diffraction patterns from thin sections of contracting rabbit skeletal muscle. Because of these observations, it is thus very likely that the intensity increase of the first actin layer-line in the *Limulus* pattern reflects structural changes upon activation common to muscles of different species.

For a long time it has been puzzling that no significant intensity increase is observed along any of the actin layer-line during contraction of frog muscle (Huxley et al., 1982). The present results for the *Limulus* pattern indicate that the actin layer-lines, especially the first (*A2*) layer-line, do indeed undergo substantial changes. This was made possible because in this muscle the actin layer-lines can be easily separated from the myosin layer-lines. In this context our results show the advantage of comparative work in the study of muscle contraction. The simpler pattern associated with *Limulus* muscle can provide information which, besides its intrinsic interest, complements the interpretation of the more complex pattern from frog muscle for which a large amount of experimental data is available.

Conclusion

On the x-ray diffraction pattern from contracting *Limulus* muscle, the intensity increase of the first actin layer-line (*A2*) has been observed. Since the intensity increase is substantial, and since the increase is highly likely associated with the actomyosin interaction, the reflexion provides a good tool for investigating the mechanism of muscle contraction and the calcium regulation. The present work also demonstrates the usefulness of an area detector used with a synchrotron radiation x-ray beam.

Y. Maéda is indebted for valuable suggestions to Drs. K. C. Holmes, R. S. Goody, J. S. Wray, and K. J. V. Poole and is also grateful to Drs. H. E. Huxley, R. M. Simmons, and the late Mr. M. Kress for encouragement and discussions.

Received for publication 21 February 1986 and in final form 12 May 1986.

REFERENCES

Bordas, J., M. H. J. Koch, P. N. Clout, E. Dorrington, C. Boulin, and A. Gabriel. 1980. A synchrotron radiation camera and data acquisition system for time resolved x-ray scattering studies. *J. Phys. E:Sci. Instrum.* 13:938–944.

Boulin, C. 1982. Calibration channel unit (CCU): a 16 channel data acquisition module with autonomous memory. *Nucl. Inst. Meth.* 201:251–259.

Boulin, C., D. Dainton, E. Dorrington, G. Elsner, A. Gabriel, J. Bordas, and M. H. J. Koch. 1982. Systems for time resolved x-ray measurements using one-dimensional and two-dimensional detectors—requirements and practical experience. *Nucl. Inst. Meth.* 201:209–220.

Clout, P. N., P. J. Bendall, and F. R. Golding. 1978. Data acquisition with a PDP-11 under RSX-11M using the CAMAC serial highway. *Proc. Digital Equipment Comp. Users Soc.* 5:247–251.

Egelman, E. H., N. Francis, and D. J. DeRosier. 1982. F-actin is a helix with a random variable twist. *Nature (Lond.).* 298:131–135.

Golding, F. R. 1982. CATY, a system for experiment control, data collection, data display, and analysis. *Nucl. Inst. Meth.* 201:231–235.

Haselgrove, J. C. 1973. X-ray evidence for a conformational change in the actin containing filaments of vertebrate striated muscle. *Cold Spring Harbor Symp. on Quant. Biol.* 37:341–352.

Hendrix, J., M. H. J. Koch, and J. Bordas. 1979. A double focusing x-ray camera for use with synchrotron radiation. *J. Appl. Cryst.* 12:467–472.

Holmes, K. C., R. T. Tregear, and J. Barrington-Leigh. 1980. *Proc. R. Soc. Lond. B. Biol. Sci.* 207:13–33.

Huxley, H. E., and W. Brown. 1967. The low-angle x-ray diagram of vertebrate striated muscle and its behavior during contraction and rigor. *J. Mol. Biol.* 30:383–434.

Huxley, H. E., A. R. Faruqi, J. Bordas, M. H. J. Koch, and J. R. Milch. 1980. The use of synchrotron radiation in time-resolved x-ray diffraction studies of myosin layer-line reflections during muscle contraction. *Nature (Lond.).* 284:140–143.

Huxley, H. E., A. R. Faruqi, M. Kress, J. Bordas, and M. H. J. Koch. 1982. Time-resolved x-ray diffraction studies of the myosin layer-line reflections during muscle contraction. *J. Mol. Biol.* 158:637–684.

Huxley, H. E., M. Kress, and R. M. Simmons. 1985. Time-resolved x-ray diffraction studies of muscle activation and contraction. *Biophys. J.* 47(2, Pt. 2):24*a*. (Abstr.)

Koch, M. H. J., and J. Bordas. 1983. X-ray diffraction and scattering on disordered systems using synchrotron radiation. *Nucl. Inst. Meth.* 206:461–469.

Maéda, Y. 1979. X-ray diffraction patterns from molecular arrangements with 38 nm periodicities around muscle thin filaments. *Nature (Lond.).* 277:670–672.

Maéda, Y. 1986. Contracting muscle — studies by x-ray diffraction using synchrotron radiation and newly developed detectors. *In* New Methods

in X-ray Absorption, Scattering and Diffraction for Applications in Structural Biology. H. D. Bartunik and B. Chance, editors. Academic Press, Inc., NY. In press.

Namba, K., K. Wakabayashi, and T. Mitsui. 1980. X-ray structure analysis of the thin filament of crab striated muscle in the rigor state. *J. Mol. Biol.* 138:1–26.

Tsukita, S., and M. Yano. 1985. Actomyosin structure in contracting muscle detected by rapid freezing. *Nature* (*Lond.*). 317:182–184.

Wray, J. S., P. J. Vibert, and C. Cohen. 1974. Cross-bridge arrangements in *Limulus* muscle. *J. Mol. Biol.* 88:363–348.

Wray, J. S., P. J. Vibert, and C. Cohen. 1978. Actin filaments in muscle: pattern of myosin and tropomyosin/troponin attachments. *J. Mol. Biol.* 124:501–521.

Yagi, N., E. J. O'Brien, and I. Matsubara. 1981. Changes of thick filament structure during contraction of frog striated muscle. *Biophys. J.* 37:121–138.